

## Observations of Pc 3-4 and Pi 2 geomagnetic pulsations in the low-latitude ionosphere

R. A. Marshall<sup>1,2</sup>, F. W. Menk<sup>1,3</sup>

<sup>1</sup> Department of Physics, the University of Newcastle, Callaghan, NSW 2308, Australia  
E-mail: physpuls3@cc.newcastle.edu.au

<sup>2</sup> IPS Radio and Space Services, PO Box 1386, Haymarket, NSW 1240, Australia

<sup>3</sup> Also at Cooperative Research Centre for Satellite Systems, Canberra, ACT, Australia

Received: 18 August 1998 / Revised: 12 July 1999 / Accepted: 20 July 1999

**Abstract.** Day-time Pc 3-4 (~5–60 mHz) and night-time Pi 2 (~5–20 mHz) ULF waves propagating down through the ionosphere can cause oscillations in the Doppler shift of HF radio transmissions that are correlated with the magnetic pulsations recorded on the ground. In order to examine properties of these correlated signals, we conducted a joint HF Doppler/magnetometer experiment for two six-month intervals at a location near  $L = 1.8$ . The magnetic pulsations were best correlated with ionospheric oscillations from near the F region peak. The Doppler oscillations were in phase at two different altitudes, and their amplitude increased in proportion to the radio sounding frequency. The same results were obtained for the O- and X-mode radio signals. A surprising finding was a constant phase difference between the pulsations in the ionosphere and on the ground for all frequencies below the local field line resonance frequency, independent of season or local time. These observations have been compared with theoretical predictions of the amplitude and phase of ionospheric Doppler oscillations driven by downgoing Alfvén mode waves. Our results agree with these predictions at or very near the field line resonance frequency but not at other frequencies. We conclude that the majority of the observations, which are for pulsations below the resonant frequency, are associated with downgoing fast mode waves, and models of the wave-ionosphere interaction need to be modified accordingly.

**Key words.** Ionosphere (ionosphere irregularities) · Magnetospheric physics (magnetosphere-ionosphere interactions) · Radio science (ionospheric physics)

### 1 Introduction

Geomagnetic pulsations are observed at the Earth's surface because magnetospheric hydromagnetic (hm) waves propagate down through the ionospheric plasma. It is well known that the ionosphere acts to modify characteristics of these downgoing waves. Effects that have been theoretically predicted and observed include rotation of the wave's polarization ellipse, and damping and filtering of the signal (e.g. Hughes and Southwood, 1976; Newton *et al.*, 1978; Andrews *et al.*, 1979; Saka *et al.*, 1980; Glassmeier, 1984; Kivelson and Southwood, 1988; Itonaga and Kitamura, 1988, 1993).

The distribution of plasma within the ionosphere can also be modified by downgoing hm waves. This is demonstrated in experiments that monitor the Doppler shift of ionospherically reflected HF CW radio transmissions. Oscillations in the Doppler shift may be observed in correspondence with magnetic field perturbations (e.g. Chan *et al.*, 1962; Davies and Baker, 1966). Several studies have also demonstrated a correlation between ionospheric Doppler oscillations and geomagnetic pulsations, including Pc 3-4 ( $7 < f < 100$  mHz) pulsations (Menk *et al.*, 1983; Jarvis and Gough, 1988; Tedd *et al.*, 1989; Menk, 1992); Pi 2 ( $7 < f < 22$  mHz) pulsations (Lewis, 1967; Klostermeyer and Röttger, 1976; Watermann, 1987; Grant and Cole, 1992; Menk, 1992; Liu *et al.*, 1991); and Pc 1 ( $0.1 < f < 5$  Hz) pulsations (Aslin *et al.*, 1991). Auroral radar observations of Pc 5 hm waves in the ionosphere are also well documented (e.g. Harang, 1939; Walker *et al.*, 1979; Waldock *et al.*, 1983).

The first attempts to model the coupling of geomagnetic field fluctuations to the ionospheric plasma were by Rishbeth and Garriott (1964) and Jacobs and Watanabe (1966). Poole *et al.* (1988) showed that for downgoing transverse Alfvén mode waves three mechanisms contribute to the ionospheric Doppler oscillation. Sutcliffe and Poole (1989, 1990) thus modelled the amplitude and phase of Doppler oscillations in vertical incidence

ionospheric records in the presence of ULF field line resonances; see also the review by Sutcliffe (1994).

At present, comparisons of these model predictions with observations remain inconclusive (e.g. Tedd *et al.*, 1989; Al'perovich *et al.*, 1991; Grant and Cole, 1992; Menk, 1992). This is mainly because of the difficulty in obtaining a statistically significant data set with sufficient resolution to investigate the amplitude and phase of Pc 3-4 pulsations simultaneously on the ground and in the ionosphere.

This work reports results of a study of ionospheric Doppler oscillations, recorded mostly in the F-region, which were correlated with Pc 3-4 and Pi 2 magnetic pulsations measured on the ground beneath the ionospheric reflection point. The study was in two parts. First, we used six months of data to investigate how local time, season and magnetic activity affect the wave-ionosphere coupling mechanism. Then we examined the spectral and cross-phase characteristics of individual events to evaluate the relationship between the amplitude and phase of the signal in the ionosphere and on the ground over a range of pulsation frequencies. A surprising result was that for pulsation signals away from the local field line resonance (FLR) frequency the phase of the ionospheric Doppler oscillations was found to consistently lead the pulsations on the ground by 30–40°, independent of local time, season or magnetoionic mode. The results suggest that these Doppler oscillations may be driven by the electric field of the down-going fast mode wave.

## 2 The experiment

### 2.1 Overview

The data presented were recorded during two six-month campaigns at a low-latitude site, near Newcastle, Australia ( $L = 1.83$ ; geomagnetic  $-42.3^\circ$ ,  $228.1^\circ$ ;  $LT = UT + 10$ ). Ionospheric Doppler oscillations observed at near-vertical incidence at two F-region altitudes were compared with day-time Pc 3-4 and night-time Pi 2 magnetic pulsations recorded simultaneously on the ground. Station locations are shown in Fig. 1. The ground-ionosphere correlation coefficients, amplitudes and phases were determined for all the joint data, with a time resolution of order 50 ms. O- and X-mode signal characteristics were also investigated. The experiment was described in detail by Menk *et al.* (1995) and is briefly outlined here.

### 2.2 Instrumentation

Ionospheric oscillations were measured using the HF CW Doppler technique described by Watts and Davies (1960) and Davies *et al.* (1962). Two HF transmitters, phase-locked to high stability oscillators, transmitted 100 W CW signals at frequencies of 3.9465 MHz (hereafter referred to as “4 MHz”) and 7.893 MHz (hereafter “8 MHz”). These were coupled via a coaxial

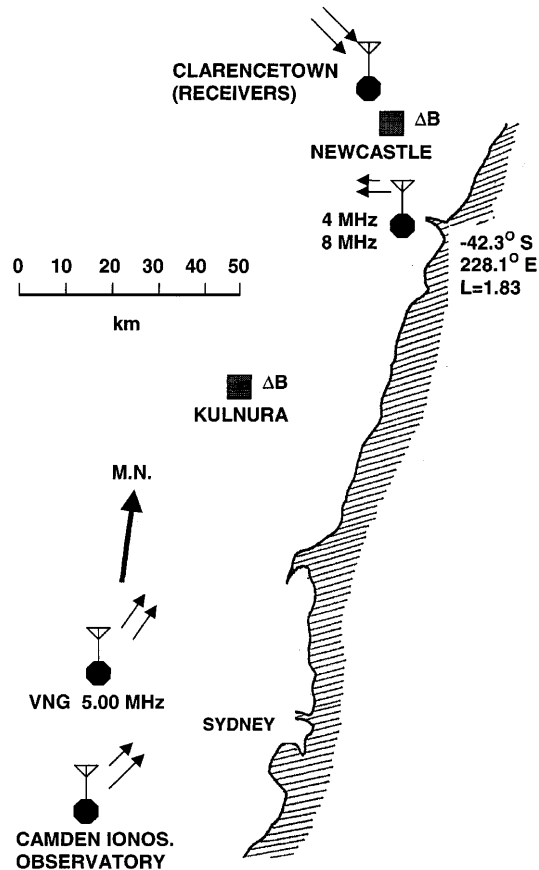


**Fig. 1.** Map showing locations of 4 and 8 MHz transmitters (Newcastle), ground magnetometer (Newcastle  $\Delta B$ ), 5.00 MHz HF Doppler transmitter (VNG) and Doppler receivers (Clarencetown). The direction of geomagnetic north is represented by M.N. The magnetometer at Kulnura was used for cross-phase determinations of the field line resonance frequency during the second campaign

bicoupler into a single trapped dipole antenna. The use of harmonically related frequencies considerably simplified design of the transmit and receive antennas.

The Doppler receivers were located about 40 km from the transmitters and used identical frequency standards. The Doppler shift in frequency of the received signals (denoted  $\Delta F_4$  and  $\Delta F_8$  respectively) was monitored using frequency-to-voltage conversion of each receiver output. Filters were used to restrict receiver bandwidth to 270 Hz and frequency response of the Doppler system to 2–300 mHz. This is optimal for studies of Pc 3-4 and Pi 2 signals in the ionosphere.

Orthogonal crossed dipole antennas and coaxial delay lines were used at the receivers to discriminate the ordinary (O) and extraordinary (X) magnetoionic modes. All data were digitized and recorded with a PC based data logger at a sample rate of 2.00 s. Timing was referenced to a standard time source, providing timing accuracy of 20–50 ms.

The entire HF transmitter-receiver system was carefully calibrated for frequency and phase response. Sensitivity of the system was such that Doppler shifts  $< 0.005$  Hz (normalized to a frequency of 1.00 MHz) could be resolved.

Geomagnetic pulsations were recorded on the ground at Newcastle beneath the ionospheric reflection point using a two-component induction magnetometer. This comprised two sensor coils of  $2 \times 10^5$  turns connected to chopper-stabilized preamplifiers, filters and main amplifiers. The sensors were aligned to geomagnetic north-south (NS) and east-west (EW), i.e. measuring  $\Delta H$  and  $\Delta D$  respectively. Magnetic feedback via secondary windings on the sensor coils provided compensation of spectral response over the 3–300 mHz frequency range. Frequency and phase response of the magnetometer was essentially identical to that of the Doppler system. The minimum detectable magnetic signal above the noise background was typically around 0.02 nT. This magnetometer is similar to instruments used by Waters *et al.* (1991, 1994) and Menk *et al.* (1995). Magnetic pulsation data were recorded using an identical PC based data logger to the Doppler system. A further 10 Doppler/magnetometer systems have subsequently been assembled for studies of the spatial characteristics of ULF pulsations, which will be reported elsewhere.

### 2.3 Data campaigns and analysis

Data recording campaigns were conducted over June–December 1991 and December 1992–July 1993. The experimental configuration described relates to the first campaign, when predominantly O-mode signals were recorded. Most of the observations presented here are from this first campaign. The second campaign used the 5.00 MHz transmitter at VNG (see Fig. 1) and the receivers at Clarendon specifically to compare the O- and X-mode signals. A second magnetometer was also operated during this campaign at Kulnura, beneath the VNG-Newcastle mid-point, and helped identify the FLR frequency using cross-phase measurements (Waters *et al.*, 1991).

Visual inspection of all the raw Doppler and magnetometer time series allowed selection of times with similar activity. From the first campaign, these were sorted into 306, 17-min intervals exhibiting simultaneous Doppler and magnetic oscillations between 0600 LT and 1700 LT. A further 39, 8.5-min intervals were obtained between 2000 LT and 0400 LT from this campaign. Next, the magnetometer-Doppler sounder cross-correlation coefficient,  $\gamma$ , was computed for all these intervals, and 281 were found to have  $\gamma \geq 0.4$ . General properties for these events, including the dependence on magnetic activity, local time and season, are outlined in Sect. 3.

The criterion  $\gamma \geq 0.6$  was then used to select events for detailed analysis. In general most power in the magnetic pulsation spectrum at these latitudes occurs at low frequencies ( $f < 40$  mHz), and FLRs are at frequencies in the range  $30 < f < 60$  mHz (Waters *et al.*, 1991). Therefore two passes were taken through the data set. In the first pass the time series were not filtered and thus lower frequency events were selected, while for the second pass data were high pass filtered at 30 mHz.

Correlated magnetic and ionospheric oscillations were sorted into the following categories:

- Day-time events (0600–1700 LT) with frequency below the local FLR frequency (i.e.  $2 \leq f \leq 40$  mHz), which we hereafter call *Pc 3-4 events*: 57 events;
- Continuous, regular day-time events with frequency  $30 < f \leq 60$  mHz, including events at or near the resonant frequency, which we call *regular Pc 3 events*: 49 events;
- Irregular night-time events (2000–0400 LT): 34 events.

For each correlated event the following parameters were then evaluated at the frequency(ies) where the cross-power (in linear units) exceeded half the maximum cross-power for the event:

- Mean amplitude of the Doppler oscillations,  $\Delta F$  (Hz);
- Mean amplitude of the magnetic pulsations,  $\Delta H$  and  $\Delta D$  (nT);
- Cross-phase between the NS magnetometer component and the Doppler oscillation ( $\Delta\phi_{NS}$ );
- Cross-phase between the EW magnetometer component and the Doppler oscillation ( $\Delta\phi_{EW}$ );
- Cross-phase between the Doppler oscillation at two different altitudes ( $\Delta\phi_{4,8}$ ).

The cross-phase was computed using a 256 point FFT for day-time events (types (a) and (b)), giving a frequency resolution of 2 mHz, or a 128 point FFT for night-time events (4 mHz resolution).

## 3 General properties

### 3.1 Ionospheric irregularities

The HF Doppler records displayed a wide variety of quasi-sinusoidal features over the Pc 3-4 range. Internal gravity waves, infrasonic acoustic waves and other travelling ionospheric disturbances cause multiple reflections of radio signals, resulting in ray interference and beating effects in Doppler records (e.g. Georges, 1967; Hooke, 1968; Davies and Jones, 1973). These are very common features and are not related to ULF magnetic pulsations. Their identification was discussed by Georges (1967), Menk (1992) and Menk *et al.* (1995), where examples were also presented.

### 3.2 Geomagnetic pulsations

During June–December 1991 over 340 intervals with simultaneous magnetic and ionospheric oscillations were recorded. Figure 2 shows unfiltered time series for a typical interval on 14 September, 1991. Short period oscillations are evident simultaneously in the ground magnetometer (NS and EW) and F-layer Doppler records (4 MHz and 8 MHz). They are in phase or nearly in phase on each trace. Oscillations such as these could persist for some hours.

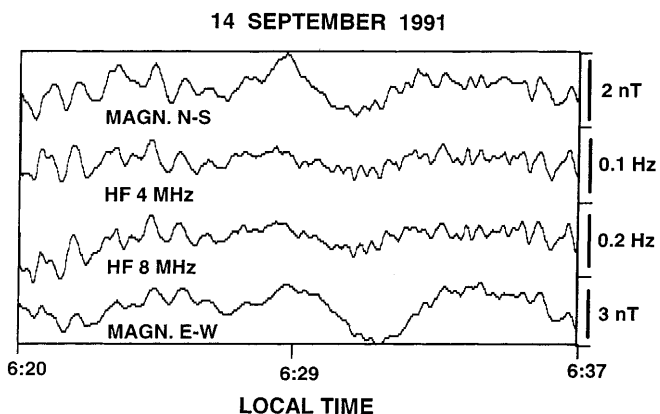


Fig. 2. Typical unfiltered record showing simultaneous oscillations in the ionospheric F-region and the ground-level magnetic field, 0620–0637 LT (= UT + 10 h), 14 September 1991. Traces are, from top to bottom: north-south magnetometer component ( $\Delta H$ ); 4 MHz ionospheric Doppler shift; 8 MHz Doppler shift; east-west magnetometer component ( $\Delta D$ )

Joint magnetic and ionospheric oscillations were observed over  $K_p$  values ranging from 1 to 9, although relative occurrence rates increased with increasing  $K_p$ . Simultaneous magnetic and ionospheric pulsations are obviously common phenomena. Ground-ionosphere correlation coefficients up to 0.9 were obtained under all magnetic conditions. Normalized Doppler shifts were in the range  $0.01 \leq (\Delta F/\Delta H) \leq 0.4$  Hz/nT. For daytime signals these correspond to vertical motions of the reflection point of a few meters to a few tens of meters, assuming no change in refractive index over the ray path. For Pi 2 events equivalent vertical displacements are up to 1–2 km.

A clear seasonal pattern was observed in the onset time and duration of correlated events. Figure 3 shows that most of the 4 MHz events occurred just after sunrise, and earlier in October/November (spring/summer months) than in June/July (winter months). The corresponding plots for 8 MHz (not presented) show that higher in the F-region events occurred later in the

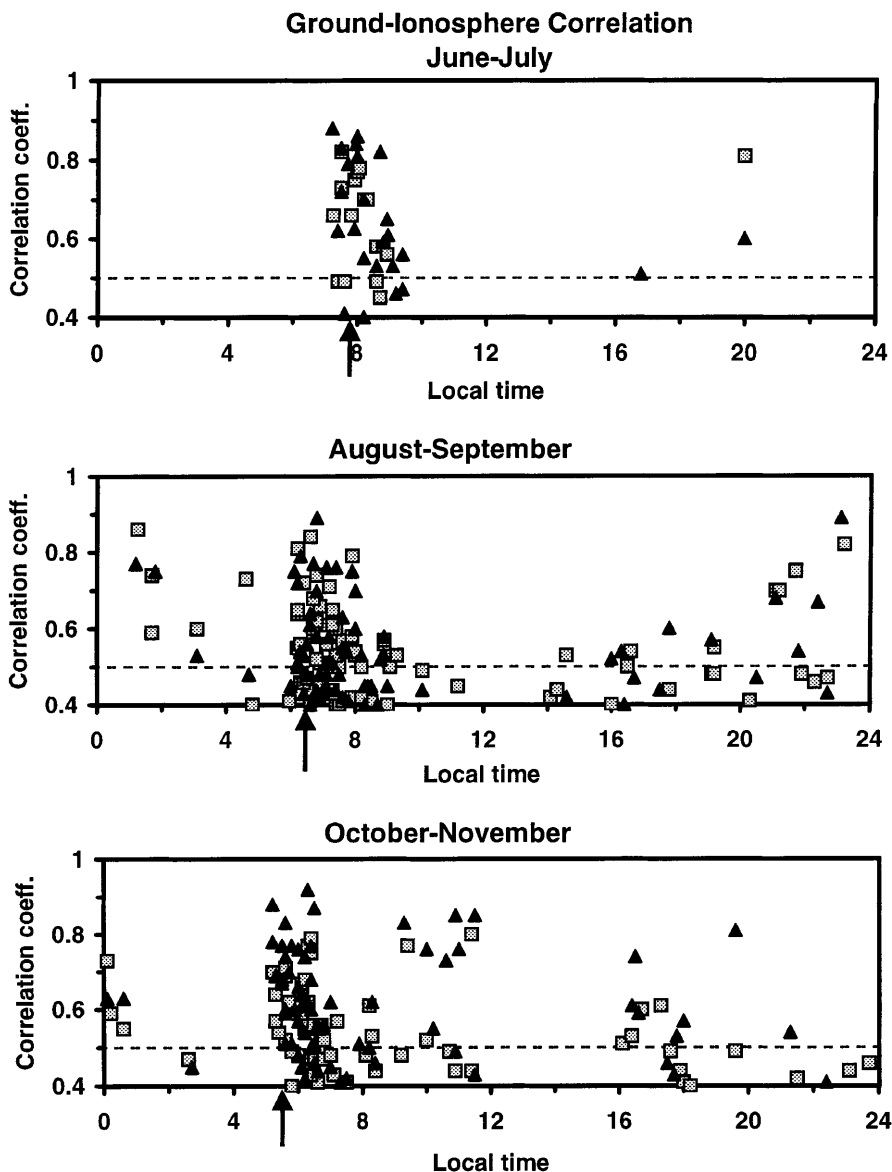


Fig. 3. Correlation coefficients for joint oscillations in the 4 MHz Doppler shift and NS (squares) and EW (triangles) ground magnetometer components, compared to local time and season. Top panel is for local winter (June/July), middle panel for equinox, and bottom panel for late spring/early summer. Arrows denote sunrise

day and had longer duration. The Doppler oscillations are therefore most likely to be observed when they occur at or just below the F-layer critical frequency. This agrees with previous studies that found that irregularities near the reflection height have the greatest effect on phase path changes (Fooks, 1962; Georges, 1967; Robinson and Dyson, 1975).

### 3.3 Case studies

To illustrate how the occurrence of ionospheric Doppler oscillations is affected by local time, season and magnetic activity, two days for which ionospheric and magnetic conditions were markedly different are presented in detail. The ionospheric data were scaled from original ionograms recorded at two sites near Canberra (denoted C in the plots) and Camden, near Sydney (denoted S), respectively located approximately 350 km and 170 km south of the Doppler sounder and magnetometer at Newcastle (see Fig. 1). The separation between these ionospheric observatories and the Doppler sounder near Newcastle means that in the following plots echoes in the Doppler records sometimes appear to come from a frequency slightly above the critical frequency. All E- and F1-region values are from the Canberra observatory.

The first day considered is 18 June, 1991, when  $K_p$  ranged from 3+ to 7+. Figure 4 shows the variation in E- and F-layer critical frequencies, ground-ionosphere correlation coefficients over the Pc 3-4 range, and ground-level pulsation activity, for the NS magnetometer component. The highest correlation coefficients generally occurred when the Doppler oscillations came from near the peak of the sporadic-E, F1- or F2-layers, even if relatively large amplitude magnetic pulsations were present at other times. Correlation coefficients for the EW magnetometer component (not shown here) were slightly higher but with the same trend.

On the second day, 20 October 1991,  $K_p$  ranged from 2 to 3+. Figure 5 presents the corresponding plots of critical frequencies, correlation coefficients and pulsation amplitude in the same format as Fig. 4. This was a day of very little pulsation activity, and F-layer critical frequencies were also significantly lower than in the previous example. However, higher ground-ionosphere correlation coefficients were sometimes obtained. This seems to be connected with the radio sounding frequency being close to  $f_oF_2$  or  $f_oE_s$  for extended periods. For example, near 0600 LT  $f_oF_2$  (C) is near 6 MHz,  $f_oF_2$  (S) is near 7 MHz, and so we infer  $f_oF_2$  at Newcastle is near 8 MHz. At this time a peak occurs in the 8 MHz (actually 7.9 MHz) ionosphere-ground correlation coefficient. There is also a peak in the 4 MHz correlation coefficients that may be related to the appearance of sporadic-E with  $f_oE_s \geq 4$  MHz. Correlations were again slightly higher for the EW magnetometer component, not shown here.

## 4 Analytical results

This section presents detailed analysis of the correlated events selected as described in Sect. 2.3. Of particular

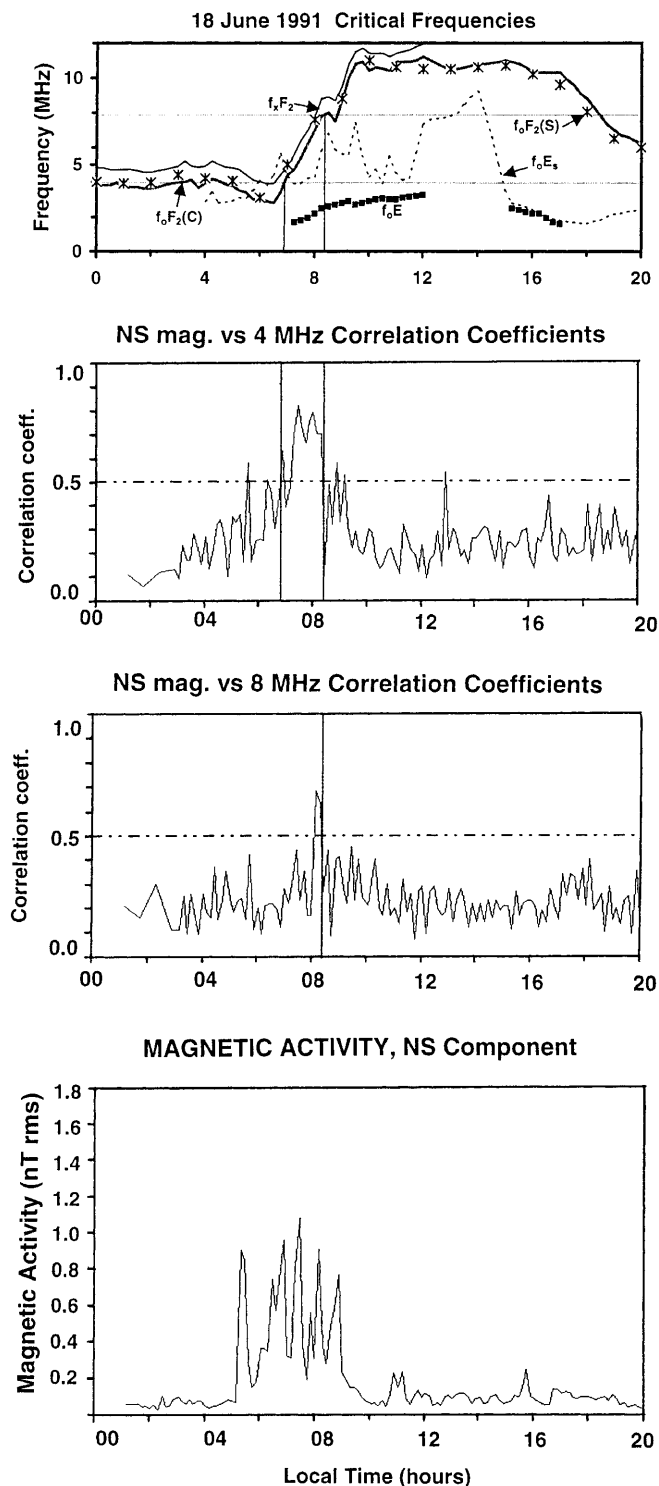


**Fig. 4.** Relationship between correlated ionospheric and magnetic oscillations and ionospheric parameters on 18 June 1991. *Top panel* shows E- and F-region critical frequencies at Canberra (C) and Sydney (S); *middle two panels* illustrate the variation in the ground-ionosphere correlation coefficients for the NS magnetic component and 4 and 8 MHz sounding frequencies; and *bottom panel* depicts the variation in pulsation activity in the NS component during this day. *Horizontal lines* indicate the two radio sounding frequencies and *vertical lines* show when  $f_oF_2$  reached these frequencies.  $K_p$  on this day ranged from 3+ to 7+

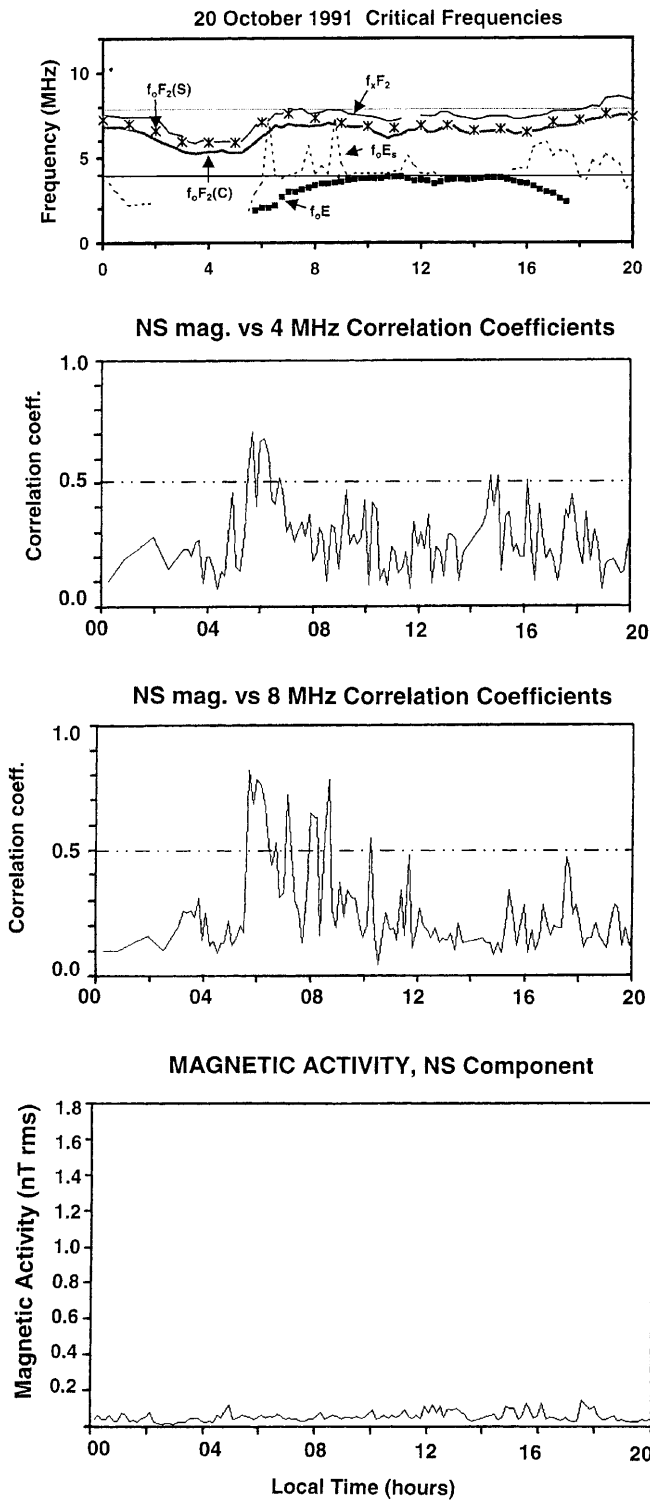


Fig. 5. As for Fig. 4, for 20 October 1991;  $K_p = 2$  to  $3+$

interest are the phase and the amplitude ratio between the geomagnetic pulsations on the ground and the Doppler oscillations in the ionosphere, and their dependence on pulsation frequency and altitude. These parameters are important for comparison with models of the coupling between ULF waves and the ionosphere, presented in Sect. 5.3.

4.1 Pc 3-4 events (2–40 mHz; 0600–1700 LT)

These magnetic pulsations are often irregular in appearance with duration from a single cycle to over an hour. They are very common at low latitudes, providing a major contribution to the pulsation spectrum. The larger oscillations evident in Fig. 2 between 0620 and 0627 LT and after 0635 LT are of this type. These would usually be denoted Pc 3-5 pulsations, although their appearance is not always of the classical, sinusoidal type.

First we consider the phase between the 4 and 8 MHz Doppler oscillations,  $\Delta\phi_{4,8}$ , corresponding typically to reflections from low and high in the F-layer. Figure 6 shows this phase difference as a function of pulsation frequency. Points with error bars denote the average of several observations, and only events with  $\gamma > 0.6$  are shown. The cross-phase values fall within  $\pm 15^\circ$  of zero phase difference. The experimental error associated with the matching of the phase responses of the Doppler systems is  $< 10^\circ$  for frequencies  $\geq 10$  mHz. At lower frequencies the instrumental mismatch becomes larger. It is clear that the Doppler oscillations were essentially in phase at different F-region altitudes. Hereafter, the 4 and 8 MHz Pc 3-4 event Doppler data have been combined for phase comparisons with the magnetometer data.

Next we examine the ground-ionosphere cross-phase,  $\Delta\phi_{EW}$ , for these signals. The variation in cross-phase with pulsation frequency for the 57 Pc 3-4 events is represented by the shaded squares in Fig. 7. Uncertainties are smaller than the symbols. A remarkably clear trend is evident. The regression line describing this relationship is  $\Delta\phi_{EW} = 0.10f - 36.8^\circ$ , with a mean standard deviation of  $\pm 27^\circ$ . A similar result was obtained for the Doppler and NS magnetometer signals,  $\Delta\phi_{NS}$ ,

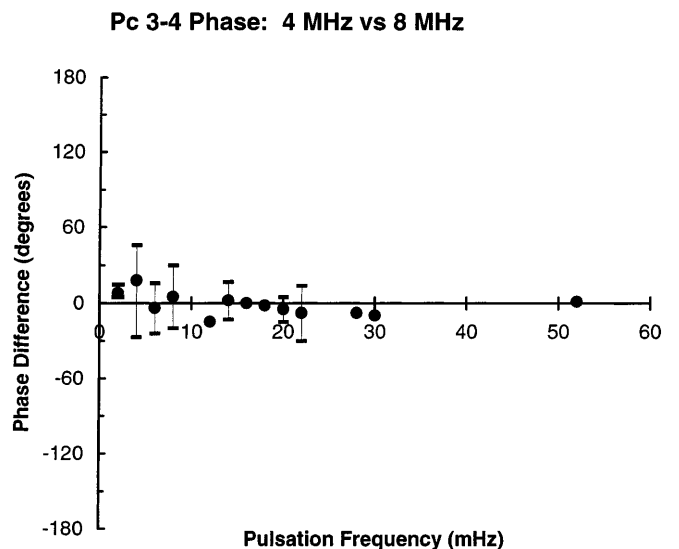


Fig. 6. Phase difference between 4 and 8 MHz Doppler shift oscillations as a function of pulsation frequency for Pc 3-4 events. Error bars denote the mean and range of several observations. Positive phase indicates the 4 MHz Doppler oscillation leading the 8 MHz oscillation

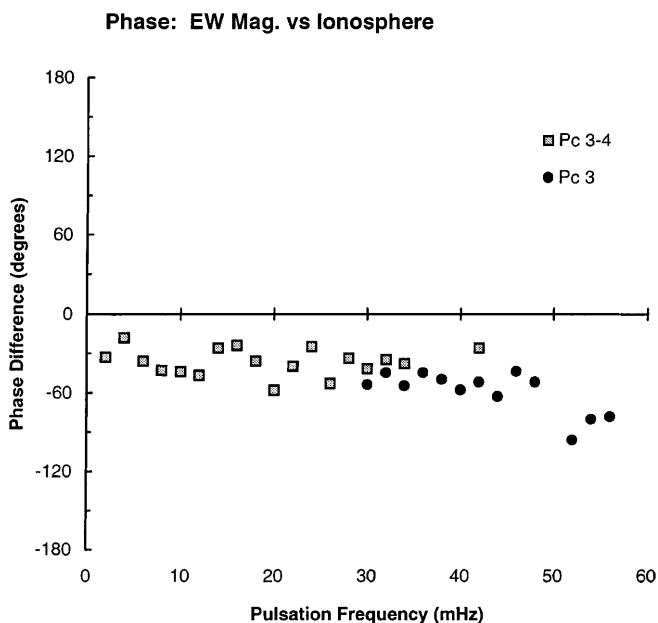


Fig. 7. Phase difference between Doppler shift oscillations and EW component magnetic pulsations as a function of pulsation frequency, for *Pc 3-4 events* (squares) and *regular Pc 3* (solid circles)

not shown here. Thus, for *Pc 3-4 events* the ground magnetometer signal consistently lagged the F-layer Doppler oscillation by around 30–40°.

Another important parameter is the magnitude of the Doppler shift,  $\Delta F$ , and its variation with altitude and magnetic pulsation frequency. The normalized Doppler oscillation amplitudes,  $\Delta F/\Delta H$  and  $\Delta F/\Delta D$ , and the 8/4 MHz Doppler shift ratios,  $\Delta F_8/\Delta F_4$ , were therefore evaluated for all events. It was found that for *Pc 3-4 events* the Doppler shift increases in proportion to the sounding frequency  $F$  (actually,  $\Delta F_8/\Delta F_4 = 2.07 - 0.003f$ , where  $f$  is the pulsation frequency in mHz). This indicates that the dependencies of  $\Delta F_8$  and  $\Delta F_4$  on  $f$  are the same. Davies *et al.* (1962) equated proportionality between  $\Delta F$  and  $f$  with predominantly vertical oscillation of the bulk ionospheric plasma; however the same form of dependence is obtained for the  $V_1$ ,  $V_2$  and  $V_3$  models of Poole *et al.* (1988).

It was also found that, to a high degree of statistical significance, the Doppler oscillation amplitude increased directly with pulsation frequency when normalized with respect to either the NS or EW magnetometer component; i.e.  $\Delta F/\Delta H \sim \Delta F/\Delta D \propto f$ , for  $2 \leq f \leq 40$  mHz.

#### 4.2 Regular *Pc 3* (30–60 mHz; local day-time)

These signals have the continuous, monochromatic, sinusoidal appearance of *regular Pc 3* pulsations and include field line resonances or quasi-resonances (Ziesolleck *et al.*, 1993; Menk *et al.*, 1994). The amplitude and structure of the NS and EW magnetometer components are often different, and the interstation phase and polarization properties are consistent with phase reversal at the resonance latitude. Examination of

cross-phase spectra from the Newcastle-Kulnura magnetometer pair for selected days during the second recording campaign confirmed that the signals we are discussing here are at resonance or near resonance (see Waters *et al.*, 1991, or Menk *et al.*, 1994, for examples of cross-phase magnetometer signatures of FLRs).

To examine the ground-ionosphere amplitude and phase properties for these pulsations the same analysis procedure was used as for the *Pc 3-4 events*. A typical interval of *regular Pc 3* activity, from 0655–0713 LT on 1 September, 1991, is illustrated in Fig. 8. The horizontal dashed line in the middle panel denotes a threshold level below which signals were considered unreliable and excluded from further analysis. Acceptable phase values are indicated by arrows in the bottom panel. Altogether 49 separate *regular Pc 3* intervals were examined in this way.

First we consider the phase relationships for these intervals. Within experimental uncertainty, the Doppler oscillations were in phase at both 4 and 8 MHz,  $\Delta\phi_{4,8} \sim 0^\circ$ , as for the *Pc 3-4 events*. The ground-ionosphere cross-phase,  $\Delta\phi_{EW}$ , as a function of pulsation frequency,  $f$ , is depicted by the filled circles in Fig. 7. The ionospheric oscillations appear to lead the magnetic oscillations by  $\sim 30$ – $60^\circ$ . The regression line is described by  $\Delta\phi_{EW} = -0.22f - 46.2^\circ$ , with a mean standard deviation of  $\pm 22^\circ$ . The significance of the points  $\geq 44$  mHz which do not obey this trend is discussed in Sect. 5.4. A similar result was also obtained for the NS magnetometer component,  $\Delta\phi_{NS}$ , although the spread in cross-phase values was greater.

Whereas for *Pc 3-4 events* the Doppler oscillation amplitude increased in direct proportion to the pulsation frequency,  $\Delta F/\Delta H \sim \Delta F/\Delta D \propto f$ , this trend was only present for *regular Pc 3* pulsations for the EW component, i.e.  $\Delta F/\Delta D \propto f$ . Doppler amplitudes normalized with respect to the NS component decreased with increasing pulsation frequency for *regular Pc 3* events; i.e.  $\Delta F/\Delta H \propto 1/f$ . The statistical significance of this trend was  $>0.99$ . These results may indicate that the NS magnetic component undergoes a different coupling mechanism with the ionospheric plasma than the EW component, or may result from the differing field geometry with respect to vertical in these two directions.

#### 4.3 Irregular night-time events (*Pi 2*, *Pc 4*; 2000–0400 LT)

The same analysis method was used for the 34 *Pi 2*/irregular *Pc 4* events recorded in the midnight sector during June–December 1991. Similar results were obtained as for day-time *Pc 3-4 events*:  $\Delta\phi_{EW} \sim 30$ – $45^\circ$ ;  $\Delta F_2/\Delta F_1 \sim 1.7$ ; and  $\Delta F/\Delta H \sim \Delta F/\Delta D \propto f$ , although the result for the EW component exhibited more scatter.

#### 4.4 O- and X-mode analysis

The purpose of the second six month recording campaign was to systematically examine Doppler pulsations

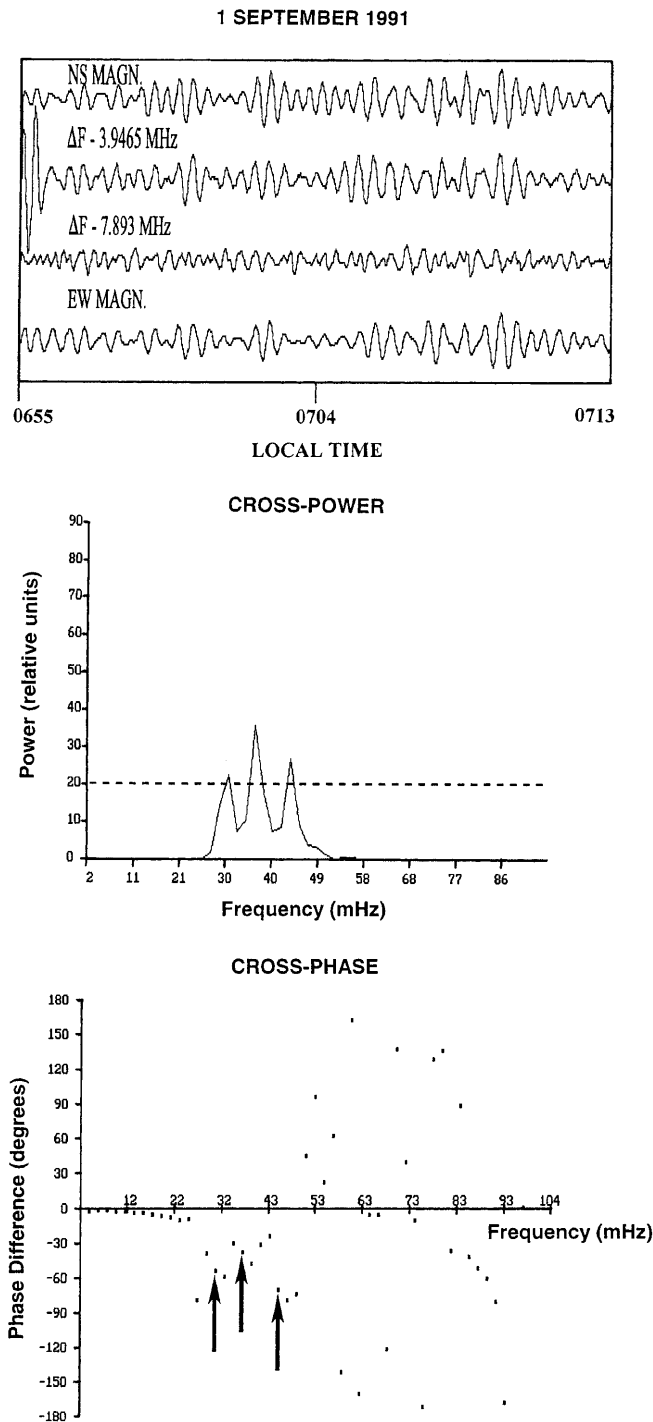


**Fig. 8.** Typical example of regular Pc 3, 1 September 1991. *Top panel* shows Doppler and magnetometer time series, highpass filtered at 30 mHz, in the same format as for Fig. 2. *Middle panel* presents EW magnetometer/4 MHz Doppler cross-power spectrum for this event; *bottom panel* shows corresponding cross-phase spectrum. Values with acceptable cross-power are *arrowed*. Negative cross-phase denotes the ground pulsation lagging the ionospheric Doppler oscillation

on the separated magnetoionic (O and X) modes. This type of experiment is hindered by the typically 20–30 dB lower amplitude of the X-mode signal compared to the O-mode. Therefore this O- and X-mode study was conducted only at a frequency of 5.000 MHz using the

more powerful VNG transmitter (Fig. 1). Detailed analysis (correlation coefficients, phase differences and amplitude variations) was performed for a total of 21 joint O- and X-mode pulsation events, of which 9 Pc 3-4 events and 5 Pi 2 events exhibited ground-ionosphere correlation coefficients  $\gamma > 0.6$ .

A typical day-time Pc 3-4 event recorded in both O- and X-modes is shown in Fig. 9. Whilst the X-mode signal was noisier, because of the lower signal level, the O- and X-mode traces are clearly of similar amplitude and phase.

A general result for all the events examined is that the O- and X-mode Doppler oscillations had similar phase and amplitude at all local times. This was confirmed using cross-phase and amplitude comparisons as described earlier. The phase difference between the O- and X-mode Doppler oscillations is shown in Fig. 10. A second independent method, peak-to-peak comparison, was also used to evaluate the signal phase. Both methods showed that there was little phase difference between the two modes, with the O-mode signal possibly lagging the X-mode signal by 8–10°. The largest differences occurred at very low frequencies ( $\leq 5$  mHz), where instrumental phase differences become significant. The same ground-ionosphere phase difference of  $\sim 45^\circ$  was also observed for both magnetoionic modes.

## 5 Summary and discussion

### 5.1 Summary

This study has provided new results on pulsation-driven ionospheric Doppler oscillations that may be compared

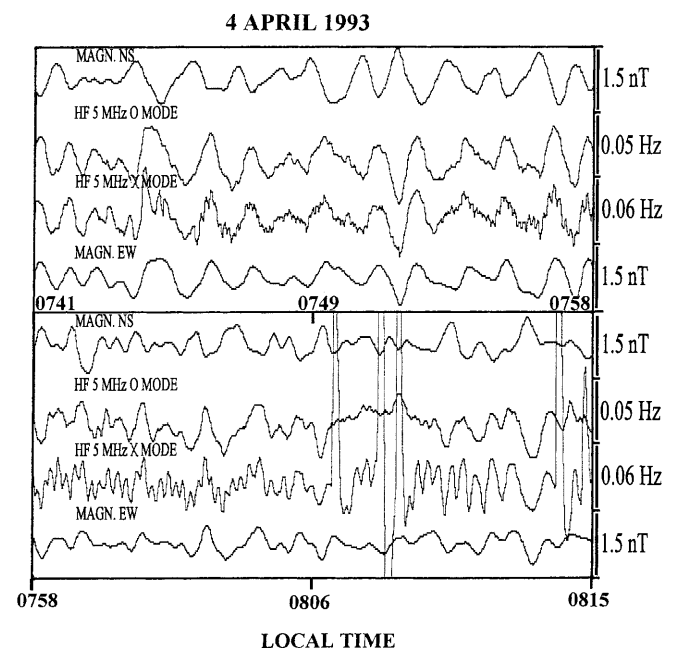


**Fig. 9.** Typical Pc 3-4 events recorded in both magnetoionic modes, 0741–0758 LT (*top panel*) and 0758–0815 LT (*bottom panel*), 4 April 1993. Traces in each panel are, from *top to bottom*: NS magnetometer component; 5.00 MHz O-mode and X-mode Doppler shifts; EW magnetometer component



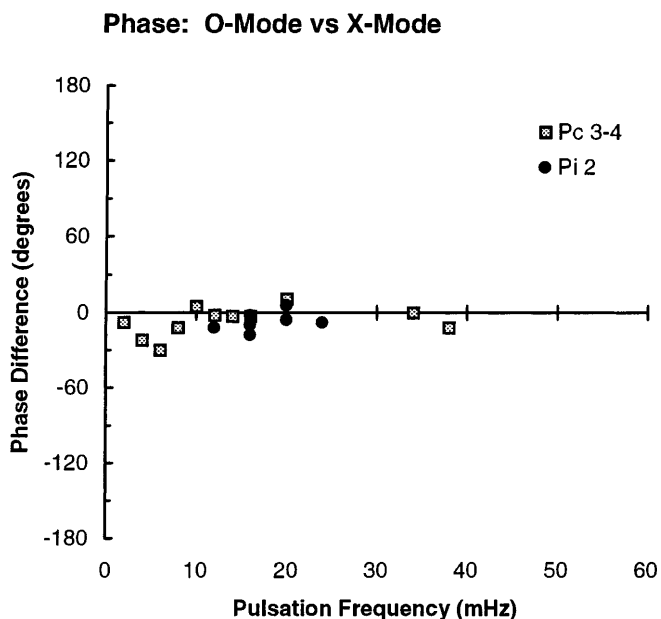


Fig. 10. Phase difference between 5.00 MHz O- and X-mode Doppler shifts. Squares denote day-time Pc 3-4 events, solid circles night-time Pi 2 events

with model predictions. The principal observational results are summarized.

1. Simultaneous Doppler oscillations and magnetic pulsations exhibit highest correlation coefficients when the radio waves are reflected from near the critical frequency in the F-layer. High correlation values may also occur for reflection from a sporadic-E layer.

2. Ground-ionosphere correlation coefficients are slightly higher when evaluated using the magnetometer D component than for the H component.

3. Correlated events may be observed at all local times (although depending on the sounding frequency they occur most often soon after sunrise) and all seasons, with similar amplitude and phase properties.

4. Doppler oscillations are in phase, or nearly in phase, at two different F-layer altitudes, for Pc 3-4 and Pi 2 pulsations.

5. The phase between the H or D magnetometer components and the Doppler oscillations is constant for all pulsations with frequency between 2 and about 44 mHz, with the ionospheric pulsations leading by 30–40°. At higher frequencies the phase difference may be much larger.

6. The ratio  $\Delta F_8/\Delta F_4$  of Doppler amplitudes is in the range 1.6–2.0 for Pc 3-4 and Pi 2 events.

7. For Pc 3-4 pulsations, Doppler shift amplitude normalized with the magnetometer D component increases with increasing pulsation frequency over the range 2–60 mHz:  $\Delta F/\Delta D \propto f$ ,  $2 \leq f \leq 60$  mHz. No trend was clear for Pi 2 events.

8. For Pc 3-4 pulsations, Doppler shift amplitude normalized with the magnetometer H component increases with pulsation frequency up to 30 mHz:  $\Delta F/\Delta H \propto f$ ,  $2 \leq f \leq 30$  mHz, but above this (i.e. approaching

and near the resonant frequency), normalized Doppler shift amplitudes decrease:  $\Delta F/\Delta H \propto 1/f$ ,  $30 \leq f \leq 60$  mHz. For Pi 2 events the rate of increase is an order of magnitude greater.

9. Phase and amplitude of the Doppler oscillations is generally independent of magnetoionic mode. However, the O-mode signals lag the X-mode signals by 8–10°.

### 5.2 Models of hm wave effects in the ionosphere

A number of modelling approaches have been used to investigate how downgoing hm waves may generate ionospheric oscillations (see review by Sutcliffe, 1994). Rishbeth and Garriott (1964) considered changes in the phase path of a radio signal due to vertical motions of the ionosphere. It was assumed these were driven by the “motor” comprising an alternating E-region electric field and associated  $\mathbf{E} \times \mathbf{B}$  plasma motion. A second mechanism proposed by them considered the sinusoidal displacement of geomagnetic field lines by propagating Alfvén waves, associating the normalized velocity of motion of the lines of force,  $\mathbf{v}/\mathbf{b}$ , with the Alfvén wave dispersion relation.

Jacobs and Watanabe (1966) considered the radio wave phase path changes to be due to changes in the refractive index of the ionosphere. These in turn were related to the vertical variation in electron density and drift velocity, driven by time variations in the north-south magnetic field or in the ionospheric electric current system.

These early models involved several limiting assumptions and did not account for the effect of the atmosphere and ionosphere on the incident hm wave (Hughes and Southwood, 1976; Glassmeier, 1984). This was addressed by Poole *et al.* (1988) and Sutcliffe and Poole (1989), who suggested the Doppler oscillations arise from the combination of four individual mechanisms. Briefly, these mechanisms account for contributions due to: (1) changes in the refractive index arising from its dependence on magnetic field intensity, requiring no bodily movement of electrons; (2) vertical motion of the electron gas under the influence of the eastward directed wave electric field; (3) currents associated with the magnetic pulsation field, compression and rarefaction of the plasma by the magnetic field, and electron motion due to the magnetic field gradient; and (4) production and loss of ionization. Poole *et al.* (1988) called these the  $V_1$ ,  $V_2$ ,  $V_3$  and  $V_4$  mechanisms respectively, following the radar convention describing the Doppler shift of a returning echo in terms of target velocity. This should not be taken to imply that the Doppler oscillations are due solely to motions of the reflection point. The production and loss mechanism ( $V_4$ ) may be ignored at the time scales and latitudes of interest here. This may not be the case at auroral or polar latitudes (Wright *et al.*, 1997).

Numerical evaluation of these mechanisms involves numerous parameters. These include the radio sounding frequency, the electron concentration profile (and hence solar cycle, season and local time), the magnetoionic

mode, magnetic dip angle, pulsation scale size, and pulsation frequency. Sutcliffe and Poole (1989, 1990) computed the amplitude and phase of the resultant Doppler oscillation,  $V^*$ , for a standard parameter set and then varied selected parameters one at a time. They assumed downgoing transverse Alfvén mode waves and evaluated the direct, Pedersen and Hall conductivities and electron mobility for a given (model) electron concentration profile, then calculated the pulsation electric and magnetic field profiles through the ionosphere for the incident wave following the method of Hughes and Southwood (1976). Sutcliffe and Poole (1989, 1990) thus modelled the amplitude and phase of Doppler oscillations in vertical incidence ionospheric records in the presence of ULF field line resonances, although the expressions themselves should have much wider applicability if evaluated for the appropriate wave mode.

### 5.3 Comparison of observations with model predictions

To facilitate comparison of our observations with the Sutcliffe and Poole (1989, 1990) model predictions, Doppler velocity amplitude and phase profiles were constructed from those of our experimental results which best match the standard parameter set used in their model computations. These parameters are listed in Table 1. Model parameters such as dip angle, time, season and solar cycle match our experimental conditions fairly well. We considered pulsations in two categories:

- (a) Regular day-time Pc 3 events near the local resonant frequency, i.e.  $\sim 50$  mHz at noon (Waters *et al.*, 1994). The observed Doppler velocities for events in the 40–50 mHz range were adjusted to give equivalent amplitude and phase values at exactly 50 mHz.
- (b) Day-time Pc 4 events with frequency  $\sim 15$  mHz. These were also adjusted to give equivalent values at exactly 15 mHz.

The results are summarized in Fig. 11, which shows the variation with altitude of our observed Doppler

velocities and phases compared to the Sutcliffe and Poole (1990) model predictions. The ordinate axes depict sounding frequency normalized by Canberra  $f_0F2$  values, thus representing crude estimates of the reflection height relative to the F2-layer peak. These values may exceed unity because at the times correlated oscillations were observed, critical frequencies at Newcastle were often higher than at Canberra, 350 km further south.

Figure 11a shows that for near-resonance frequencies (50 mHz), the magnitude of the Doppler velocity in the F-region compares well with model predictions of the magnitude of  $V^*$ . However, the manner in which the observed Doppler velocity varies with altitude seems to fall somewhere between predictions for the  $V_2$  and  $V_3$  mechanisms. For the day-time Pc 4 (15 mHz) events, well below the resonant frequency, the Doppler amplitudes shown in Fig. 11a are significantly larger than the model predictions (which are for 50 mHz) and do not follow a clear trend with altitude. Figure 8 of Sutcliffe and Poole (1990) shows that Doppler velocity is expected to increase with increasing pulsation frequency above  $\sim 20$  mHz, although by not as much as we have observed.

The variation in Doppler velocity phase with altitude is presented in Fig. 11b, in the same format as for Fig. 11a. The principal feature is the nearly constant ground-ionosphere phase for the observations at both 50 and 15 mHz, which does not agree with the overall model predictions,  $V^*$ . The observations appear to best approximate predictions for the  $V_2$  mechanism.

In a similar manner we have also compared the observed variation in Doppler velocity and phase with pulsation frequency, with the Sutcliffe and Poole (1990) model predictions. These are shown in Fig. 12. As before, the model predictions apply to the specific parameter set described in Table 1, whereas the observations likely encompass a wider variety of conditions. In particular, the models are very sensitive to north-south pulsation scale length. This is highly variable from one pulsation event to another, but we expect is typically of order 200–250 km at resonance (Menk *et al.*, 1994).

**Table 1.** Parameter set used for Figs. 11 and 12

Parameter	Sutcliffe and Poole (1989) modelling	Observations
Dip angle	$I = +60^\circ$	$I = -63^\circ$
Background field	$B = 30,000$ nT	$B = 56,970$ nT
Pulsation period	$T = 20$ s (50 mHz)	(a) $40 \leq f \leq 50$ mHz, normalized to 50 mHz (b) $f \sim 15$ mHz (67 s)
NS scale length	$L_x = 500$ km	Typically 200–250 km
EW scale length	$L_y = 6000$ km	Typically $3 \leq m \leq 10$
Magnetoionic component	O-mode	O-mode
NS pulsation amplitude at the ground	1 nT	Normalized to 1 nT
Pulsation phase at the ground	$0^\circ$	$0^\circ$
Local time	Midday	Mostly morning
Season	Summer	Spring
Solar cycle	Sunspot maximum	Sunspot maximum

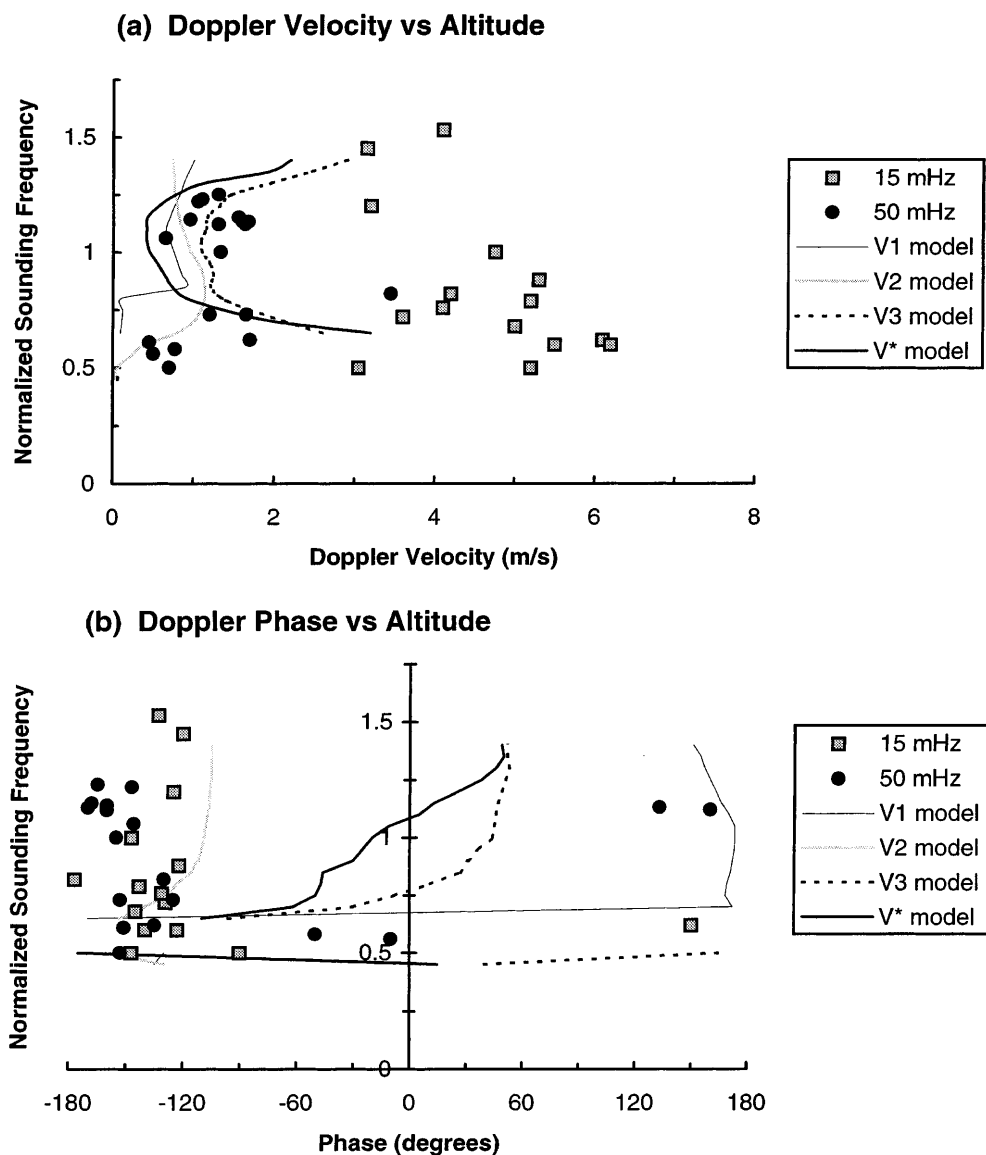


**Fig. 11a, b.** Variation of **a** Doppler velocity and **b** phase with normalized sounding frequency (i.e. altitude). Observations for 50 mHz Pc 3 (*solid circles*) and 15 mHz Pc 4 (*squares*) are compared with Sutcliffe and Poole (1990) model predictions as per Table 1

Nevertheless, clear trends are apparent in the results. The most prominent features evident in Fig. 12a are:

1. For the EW magnetometer component, the Doppler velocity increases with increasing frequency;
2. For the NS magnetometer component, the Doppler velocity peaks around 30 mHz;
3. The magnitudes of the observed Doppler velocities exceed the model predictions, approaching reasonable agreement only for the NS magnetometer component >44 mHz. The model V<sub>1</sub> contribution is negligible. Sutcliffe and Poole’s (1990) predictions show that Doppler amplitude will be an order of magnitude greater for  $L_x = 200$  km compared to  $L_x = 500$  km, and this may at least partly explain result (3).

From Fig. 12b it is again evident that the observed phase between the Doppler velocity oscillations and the magnetic pulsations was nearly constant at frequencies <44 mHz and for both magnetometer components.

There are some points  $\geq 44$  mHz for which this does not apply. It was also apparent in Figs. 7 and 11 that some points  $\geq 44$  mHz differ from the general trends. This is discussed next.

#### 5.4 Observed wave modes and model limitations

Sutcliffe and Poole (1990) demonstrated how their model predictions are affected by variations in key parameters, in particular the pulsation frequency, the pulsation NS scale size  $L_x$  and its sign (i.e. propagation equatorward or poleward). However, the most serious limitation is the assumption that the incident hm waves are purely transverse Alfvén mode. While this may be the case for pure FLRs, there is accumulating evidence that low- and mid-latitude magnetometer records contain significant spectral contributions due to cavity mode resonances, fast mode propagating waves, and coupled wave modes (e.g. Yumoto, 1985; Kivelson and

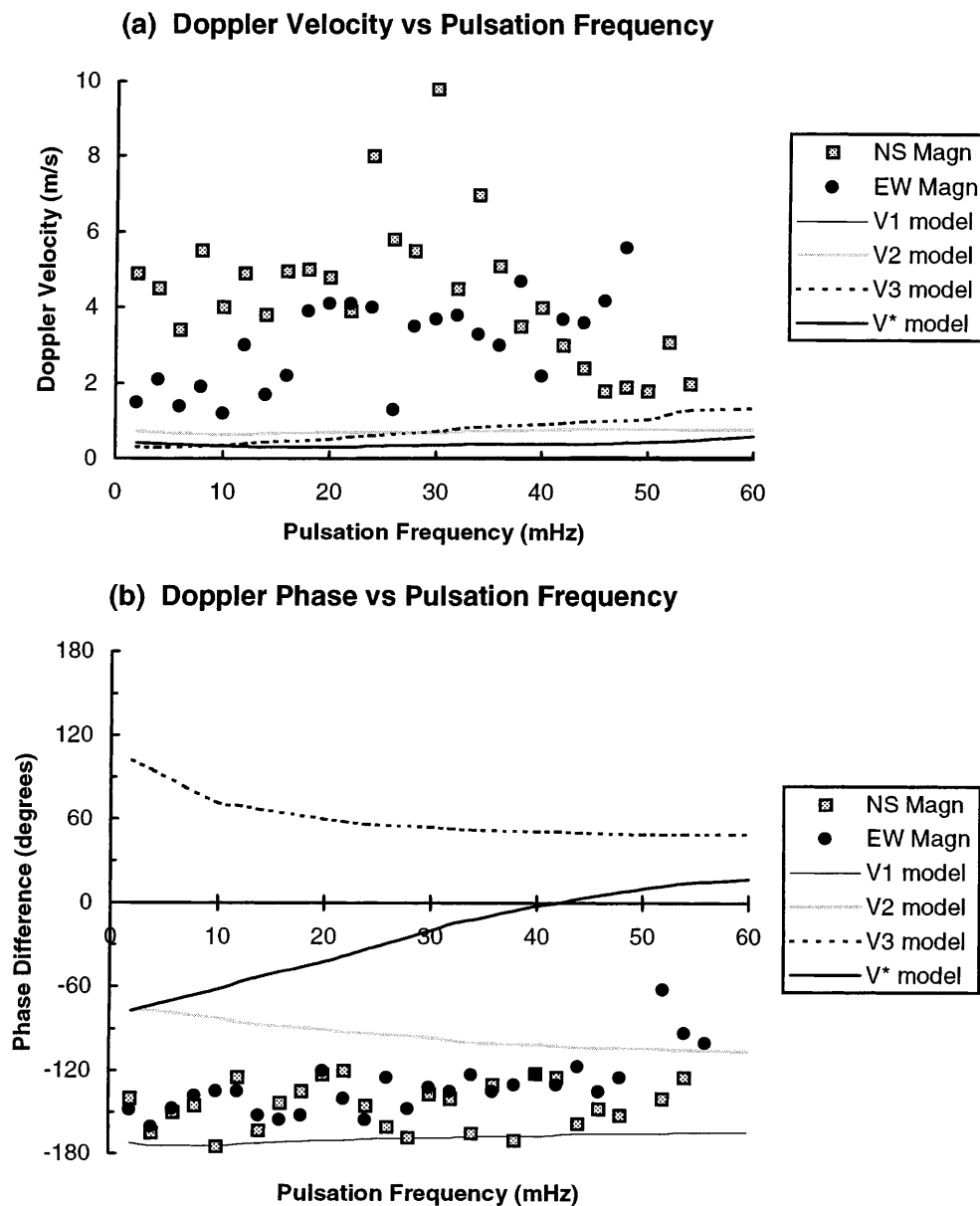


**Fig. 12a, b.** Variation of **a** Doppler velocity and **b** phase with pulsation frequency. Observations are compared with Sutcliffe and Poole (1990) model predictions; *symbols* as in Fig. 11

Southwood, 1986; Samson *et al.*, 1995). In fact, the non-localized compressional or fast mode and the localized toroidal or shear Alfvén mode always couple in a non-uniform plasma if any wave disturbances are not fully axisymmetric.

Recently, Zhang and Cole (1994) computed the electromagnetic wave amplitude and phase profiles below 500 km altitude for the general case including upgoing and downgoing Alfvén and fast mode waves. A more detailed report includes plots of all these altitude profiles (Fast and Alfvén modes of ULF electromagnetic waves in a stratified ionosphere by the method of boundary value problem, D. Y. Zhang and K. D. Cole, La Trobe University, Victoria, Australia, 1991). The equatorial case was considered in Zhang and Cole (1995). The fast mode wave profiles in both the high- and low-latitude cases are significantly different than for transverse Alfvén waves. As the model expressions for

$V_1$ ,  $V_2$  and  $V_3$  each contain one or more of the wave field  $\mathbf{E}$  and  $\mathbf{b}$  components, both the magnitude and shape of the predicted Doppler velocity profiles will be different for the two modes.

It is generally acknowledged that the amplitude and frequency of low-latitude Pc 3-4 magnetic pulsations are controlled by parameters of the solar wind and IMF, and this is regarded as evidence that ULF wave energy propagates to low altitudes in the fast mode (e.g. Yumoto, 1985; Odera, 1986). Field line resonances occur when the frequency of the incoming waves matches the local field line eigenfrequency, and are excited almost continuously during local day-time (Waters *et al.*, 1991). In ground data, FLRs are characterized by a peak in amplitude and a change in phase of the NS magnetometer component across the resonance latitude (Orr, 1984). Away from the resonance latitude the signals resemble fast mode waves in most respects,

with large horizontal scale sizes (Kivelson and Southwood, 1986; Zhang and Cole, 1994). East-west scale sizes relate to the azimuthal wave number,  $m$ , which for resonances at  $L = 1.8$  are  $m \leq 10$ , i.e.  $\sim 10^4$  km (Ansari and Fraser, 1986).

North-south scale sizes have been measured by a number of methods, and at resonance are typically of order 200–250 km (Walker *et al.*, 1979; Ziesolleck *et al.*, 1993; Menk *et al.*, 1994; Waters *et al.*, 1994), depending on the resonance Q. Wright *et al.* (1998) presented a study examining a Pc 5 ( $\sim 4$  mHz frequency) event recorded at high latitudes with a magnetometers, an HF Doppler sounder and the EISCAT UHF radar. The resonance exhibited a north-south scale size of order 500 km but the Alfvénic region of the pulsation extended some distance ( $\sim 8^\circ$ ) away from resonance. Wright *et al.* (1998) concluded the Doppler oscillations were consistent with  $\mathbf{E} \times \mathbf{B}$  effects caused by the electric field perturbation of the ULF wave.

At least some of the 50 mHz events plotted in Fig. 11 correspond to the points near 50 mHz in Figs. 7 and 12 which fall outside the general trends. Since these events are at or near the resonant frequency we expect the model predictions to be realistic. Moving away from the resonant frequency the downgoing wave will become a mixture of Alfvén and fast modes. Most of the *regular Pc 3* (30–60 mHz, local day-time) signals discussed in Sect. 4.2 are expected to fall into this category. In terms of the models, the  $V_2$  mechanism (vertical ionospheric motion) seems to best fit the observations. However this fit is approximate and this mechanism alone does not satisfactorily predict observed amplitudes and phases across a range of pulsation frequencies. The observation that Doppler shift amplitudes and phases are similar for both magnetoionic modes also tends to discriminate against the  $V_1$  (magnetic) mechanism predictions of Sutcliffe and Poole (1990).

At low latitudes significant pulsation power occurs well below the resonant frequency. These signals are generally in phase or nearly in phase at latitudinally spaced ground stations (Ziesolleck *et al.*, 1993; Matsuoka *et al.*, 1997) and are probably due to forced field line oscillations (Orr, 1984) driven by incoming global or fast mode waves. The *Pc 3-4 events* (2–40 mHz) discussed in Sect. 4.1 are most likely of this type. A surprising and very consistent result for these is the simple phase relationship between the Doppler oscillations and the magnetic pulsations, particularly evident in Fig. 12b. This relationship is independent of season, local time, altitude, and wave frequency. This is another reason why the model predictions, including that for the  $V_2$  mechanism, are not appropriate. Rather, it is necessary to invoke a model that incorporates both downgoing fast and Alfvén mode waves, varying the mixture and scale size of these with proximity to the resonant frequency. For pulsations well below the resonant frequency the wave properties are most probably dominated by the fast mode. In that case the majority of the observed Doppler shifts are likely driven by the electric field of the downgoing fast mode wave. Such modelling has now been achieved in a related study and

will be described in detail in a future paper. For signals exactly at resonance the Sutcliffe and Poole (1990) models are expected to satisfactorily explain the signal properties.

Recent experimental and theoretical studies of low-latitude Pi 2 pulsations (Sutcliffe and Yumoto, 1989; Allan *et al.*, 1996) have concluded that these are most likely due to forced field line oscillations driven by global cavity modes in the nightside. Accordingly, these signals also exhibit very large scale sizes, low azimuthal wave numbers, and latitude-independent frequency. Thus, their Doppler shift signatures are expected to be similar to those for *Pc 3-4 events* well below the resonant frequency.

The final point concerns the possible small phase difference between the O- and X-mode Doppler oscillations. The O- and X-mode radio waves propagate along different paths in the ionosphere, and therefore their reflection points are slightly separated. The O-mode ray will be reflected at a higher latitude than the X-mode, and for resonances this will result in the X-mode signal leading the O-mode (Wright *et al.*, 1997). However, since our O- and X-mode results are mostly for signals below the resonant frequency, it is not clear how this mechanism can account for the observed small phase difference.

*Acknowledgements.* This work was supported by the Australian Research Council and the University of Newcastle. RAM received financial assistance from a Space Physics Group (University of Newcastle) scholarship. Canberra and Sydney (Camden) ionospheric data were kindly supplied by IPS Radio and Space Services, Sydney. We thank P. W. McNabb for assistance with design and construction of the Doppler systems.

Topical Editor K.-H. Glassmeier thanks P. Sutcliffe and T.K. Yeoman for their help in evaluating this paper.

## References

- Allan, W., F. W. Menk, B. J. Fraser, Y. Li, and S. P. White, Are low-latitude Pi 2 pulsations cavity/waveguide modes?, *Geophys. Res. Lett.*, **23**, 765, 1996.
- Ansari, I. A., and B. J. Fraser, A multistation study of low latitude Pc 3 geomagnetic pulsations, *Planet. Space Sci.*, **34**, 519, 1986.
- Al'Perovich, L. S., E. N. Federov, A. V. Volgin, V. A. Pilipenko, and S. N. Pokhilko, Doppler sounding as a tool for the study of the mhd wave structure in the magnetosphere, *J. Atmos. Terr. Phys.*, **53**, 581, 1991.
- Andrews, M. K., L. J. Lanzerotti, and M. C. MacLennan, Rotation of hydromagnetic waves between the magnetosphere and the ground, *J. Geophys. Res.*, **84**, 7267, 1979.
- Aslin, P. M., M. J. Jarvis, and K. Morrison, Ionosonde signatures of Pc 1 pulsations, *J. Atmos. Terr. Phys.*, **53**, 33, 1991.
- Chan, K. L., D. P. Kanellakos, and O. G. Villard, Jr., Correlation of short period fluctuations of the Earth's magnetic field and instantaneous frequency measurements, *J. Geophys. Res.*, **67**, 2066, 1962.
- Davies, K., and D. M. Baker, On frequency variations of ionospherically propagated HF radio signals, *Radio Sci.*, **1**, 545, 1966.
- Davies, K., and J. E. Jones, Three dimensional observations of travelling ionospheric disturbances, *J. Atmos. Terr. Phys.*, **35**, 1737, 1973.

- Davies, K., J. M. Watts, and D. H. Zacharisen**, A study of F2-layer effects as observed with a Doppler technique, *J. Geophys. Res.*, **67**, 601, 1962.
- Fooks, G. F.**, Ionospheric irregularities and the phase path of radio waves, *J. Atmos. Terr. Phys.*, **24**, 937, 1962.
- Georges, T. M.**, Ionospheric effects of atmospheric waves, *ESSA Technical Rep. IER 57-ITSA* **54**, 1967.
- Glassmeier, K.-H.**, On the influence of ionospheres with non-uniform conductivity distribution on hydromagnetic waves, *J. Geophys.*, **54**, 125, 1984.
- Grant, I. F., and K. D. Cole**, The height dependence of the perturbation of the mid-latitude F-region by Pi 2 pulsations, *Planet. Space Sci.*, **40**, 1461, 1992.
- Harang, L.**, Pulsations in an ionized region at a height of 650–800 km during the appearance of giant pulsations in the geomagnetic records, *Terr. Magn. Atmos. Elect.*, **44**, 17, 1939.
- Hooke, W. H.**, Ionospheric irregularities produced by internal atmospheric gravity waves, *J. Atmos. Terr. Phys.*, **30**, 795, 1968.
- Hughes, W. J., and D. J. Southwood**, An illustration of modification of geomagnetic pulsation structure by the ionosphere, *J. Geophys. Res.*, **81**, 3241, 1976.
- Itonaga, M., and T. I. Kitamura**, Effect of non-uniform ionospheric conductivity distributions on Pc 3-4 magnetic pulsations-Alfvén wave incidence, *J. Geomagn. Geoelectr.*, **40**, 1413, 1988.
- Itonaga, M., and T. I. Kitamura**, Effect of non-uniform conductivity distributions on Pc 3-5 magnetic pulsations-fast wave incidence, *Ann. Geophysicae.*, **11**, 366, 1993.
- Jacobs, J. A., and T. Watanabe**, Doppler frequency changes in radio waves propagating through a moving ionosphere, *Radio Sci.*, **1**, 257, 1966.
- Jarvis, M. J., and H. Gough**, Digital ionosonde observations of Pc 3-4 pulsations across the plasmopause, *Planet. Space Sci.*, **36**, 733, 1988.
- Kivelson, M. G., and D. J. Southwood**, Coupling of global magnetospheric MHD eigenmodes to field line resonances, *J. Geophys. Res.*, **91**, 4345, 1986.
- Kivelson, M. G., and D. J. Southwood**, Hydromagnetic waves and the ionosphere, *Geophys. Res. Lett.*, **15**, 1271, 1988.
- Klostermeyer, J., and J. Röttger**, Simultaneous geomagnetic and ionospheric oscillations caused by hydromagnetic waves, *Planet. Space Sci.*, **24**, 1065, 1976.
- Lewis, T. J.**, The association of phase changes of ionospheric-propagating radio waves and geomagnetic variations, *Can. J. Phys.*, **45**, 1549, 1967.
- Liu, J. Y., Y. N. Huang, and F. T. Berkey**, The phase relationship between ULF geomagnetic pulsations and HF-Doppler oscillations owing to the compressional mechanism, *J. Geomagn. Geoelectr.*, **43**, 777, 1991.
- Matsuoka, H., K. Takahashi, S. Kokubun, K. Yumoto, T. Yamamoto, S. I. Solov'yev, and E. F. Vershinin**, Phase and amplitude structure of Pc 3 magnetic pulsations as determined from multipoint observations, *J. Geophys. Res.*, **102**, 2391, 1997.
- Menk, F. W.**, Characterisation of ionospheric Doppler oscillations in the Pc 3-4 and Pi 2 magnetic pulsation frequency range, *Planet. Space Sci.*, **40**, 495, 1992.
- Menk, F. W., K. D. Cole, and J. C. Devlin**, Associated geomagnetic and ionospheric variations, *Planet. Space Sci.*, **31**, 569, 1983.
- Menk, F. W., C. L. Waters, C. W. S. Ziesolleck, B. J. Fraser, S. H. Lee, and P. W. McNabb**, Ground measurements of low latitude magnetospheric field line resonances, in *Solar wind sources of magnetospheric ULF waves* Eds. M. J. Engebretson, K. Takahashi and M. Scholer, *Geophys. Mono.* **81**, AGU, Washington D.C., 299, 1994.
- Menk, F. W., R. A. Marshall, P. W. McNabb, and I. S. Dunlop**, An experiment to study the effects of geomagnetic fluctuations on ionospheric HF radio paths, *J. Elec. Electr. Eng. Aust.*, **15**, 325, 1995.
- Newton, R. S., D. J. Southwood, and W. J. Hughes**, Damping of geomagnetic pulsations by the ionosphere, *Planet. Space Sci.*, **26**, 201, 1978.
- Odera, T. J.**, Solar wind controlled pulsations: a review, *Rev. Geophys.*, **24**, 55, 1986.
- Orr, D.**, Magnetospheric hydromagnetic waves: their eigenperiods, amplitudes and phase variations, a tutorial introduction, *J. Geophys.*, **55**, 76, 1984.
- Poole, A. W., P. R. Sutcliffe, and A. D. M. Walker**, The relationship between ULF geomagnetic pulsations and ionospheric Doppler oscillations: derivation of a model, *J. Geophys. Res.*, **93**, 14 656, 1988.
- Rishbeth, H., and O. K. Garriott**, Relationship between simultaneous geomagnetic and ionospheric oscillations, *Radio Sci. J. Res. NBS*, **68D**, 339, 1964.
- Robinson, I., and P. L. Dyson**, Effects of ionospheric irregularities on radio waves – I: Phase path changes, *J. Atmos. Terr. Phys.*, **37**, 1459, 1975.
- Saka, O., T.-T. Iijima, and T. Kitamura**, Ionospheric control of low latitude geomagnetic micropulsations, *J. Atmos. Terr. Phys.*, **42**, 517, 1980.
- Samson, J. C., C. L. Waters, F. W. Menk, and B. J. Fraser**, Fine structure in the spectra of low latitude field line resonances, *Geophys. Res. Lett.*, **22**, 2111, 1995.
- Sutcliffe, P. R.**, Modelling the ionospheric signatures of geomagnetic pulsations, *J. Geomagn. Geoelectr.*, **46**, 1011, 1994.
- Sutcliffe, P. R., and A. W. V. Poole**, Ionospheric Doppler and electron velocities in the presence of ULF waves, *J. Geophys. Res.*, **94**, 13 505, 1989.
- Sutcliffe, P. R., and A. W. V. Poole**, The relationship between ULF geomagnetic pulsations and ionospheric Doppler oscillations: model predictions, *Planet. Space Sci.*, **38**, 1581, 1990.
- Sutcliffe, P. R., and K. Yumoto**, Dayside Pi 2 pulsations at low latitudes, *Geophys. Res. Lett.*, **16**, 887, 1989.
- Tedd, B. L., K. D. Cole, and P. L. Dyson**, The association between ionospheric and geomagnetic pulsations in the Pc 3-4 range at mid-latitudes, *Planet. Space Sci.*, **37**, 1079, 1989.
- Waldock, J. A., T. B. Jones, E. Neilsen, and D. J. Southwood**, First results of micropulsation activity observed by SABRE, *Planet. Space Sci.*, **31**, 573, 1983.
- Walker, A. D. M., R. A. Greenwald, W. F. Stuart, and C. A. Green**, STARE auroral radar observations of Pc 5 geomagnetic pulsations, *J. Geophys. Res.*, **84**, 3373, 1979.
- Watermann, J.**, Observations of correlated ULF fluctuations in the geomagnetic field and in the phase path of ionospheric HF soundings, *J. Geophys.*, **61**, 39, 1987.
- Waters, C. L., F. W. Menk, and B. J. Fraser**, The resonance structure of low latitude Pc 3 geomagnetic pulsations, *Geophys. Res. Lett.*, **18**, 2293, 1991.
- Waters, C. L., F. W. Menk, and B. J. Fraser**, Low latitude geomagnetic field line resonance: experiment and modeling, *J. Geophys. Res.*, **99**, 17 547, 1994.
- Watts, J. M., and K. Davies**, Rapid frequency analysis of fading radio signals, *J. Geophys. Res.*, **65**, 2295, 1960.
- Wright, D. M., T. K. Yeoman, and P. J. Chapman**, High-latitude HF Doppler observations of ULF waves: 1. Waves with large spatial scale sizes, *Ann. Geophysicae.*, **15**, 1548, 1997.
- Wright, D. M., T. K. Yeoman, and J. A. Davies**, A comparison of EISCAT and HF Doppler observations of a ULF wave, *Ann. Geophysicae.*, **16**, 1190, 1998.
- Yumoto, K.**, Low frequency upstream waves as a probable source of low-latitude Pc 3-4 magnetic pulsations, *Planet. Space Sci.*, **33**, 239, 1985.
- Zhang, D. Y., and K. D. Cole**, Some aspects of ULF electromagnetic wave relations in a stratified ionosphere by the method of boundary value problem, *J. Atmos. Terr. Phys.*, **56**, 681, 1994.
- Zhang, D. Y., and K. D. Cole**, Formulation and computation of hydromagnetic wave penetration into the equatorial ionosphere and atmosphere, *J. Atmos. Terr. Phys.*, **57**, 813, 1995.
- Ziesolleck, C. W. S., B. J. Fraser, F. W. Menk, and P. W. McNabb**, Spatial characteristics of low-latitude Pc 3-4 geomagnetic pulsations, *J. Geophys. Res.*, **98**, 197, 1993.